Available online at www.sciencedirect.com
ScienceDirect
Polymer 49 (2008) 1961–1967
polymer
www.elsevier.com/locate/polymer

Thickness-dependent crystal orientation in poly(trimethylene 2,6-naphthalate) films studied with GIWAXD and RA-FTIR methods

Yongri Liang[1], Meizhu Zheng, Ki Ho Park, Han Sup Lee*

Department of Textile Engineering, INHA University, 253 Young-hyun-dong, Nam-Gu, Incheon 402-751, Republic of Korea

Received 26 July 2007; received in revised form 31 January 2008; accepted 3 February 2008
Available online 13 February 2008

Abstract

The thickness dependence of the crystal orientation of poly(trimethylene 2,6-naphthalate) (PTN) films was clearly demonstrated using the methods of two-dimensional grazing incidence wide angle X-ray diffraction (2D GIWAXD) and grazing incidence reflection absorption FTIR (RA-FTIR) spectroscopy. The 2D GIWAXD results showed that for films thicker than 200 nm, the "*c*" axis (main chain direction) and "*b*" axis of crystal unit cell are almost parallel to the sample surface, whereas for thin films the "*c*" axis is preferentially perpendicular to the film plane in the crystalline phase of isothermally crystallized PTN films. The anisotropic orientation of the naphthalene rings in the isothermally crystallized PTN film was also confirmed. By analyzing the relative absorbance of the parallel band (1602 cm^{-1}) to the one of perpendicular band (917 cm^{-1}), the thickness dependence of the crystal orientation suggested by the GIWAXD results was also confirmed. Furthermore, the naphthalene rings in the isothermally crystallized thick films were found to lie flat on the film plane. The chain orientations derived from the GIWAXD and RA-FTIR results in this work were found to be consistent with the "flat-on" and "edge-on" lamellar orientation for the thin and thick films, respectively, which has previously been reported in many polymer systems.

Keywords: Poly(trimethylene 2,6-naphthalate); Crystal orientation; RA-FTIR

1. Introduction

Polymer thin and ultrathin films have received a great deal of attention both scientifically and technologically due to their usefulness for photolithography [1], liquid crystal displays [2], sensors [3], microelectronic applications [4], and antireflection coatings [5]. Given that many properties of thin polymeric materials are highly affected by the presence of surfaces and/or interfaces, a fundamental understanding of the influence of these factors on the structural aspects of polymers, such as their conformation, orientation and the local packing is essential. With ultrathin films, the glass transition temperature [6], crystallization kinetics [7,8], crystallinity [9], morphology [10] and electrical properties [4] have been reported to be highly dependent on the thickness of these films.

Schönherr et al. [10] found that for isothermally crystallized thin and ultrathin films of poly(ethylene oxides) on oxidized silicon substrates, lamellar crystals were observed to grow preferentially in "flat-on" orientation in films thinner than approximately 300 nm; i.e., the helical PEO chains are oriented along the surface normal direction. In contrast, lamellar crystals in films thicker than 1 μm are preferentially in an "edge-on" orientation. Recently, Wang et al. [9] found that the morphology of melt-crystallized LLDPE showed "edge-on" lamellae for films thicker than 30 nm and "flat-on" lamellae for films thinner than 15 nm.

Grazing incidence wide angle X-ray diffraction (GIWAXD) [11–26] and small-angle X-ray scattering (GISAXS) [26–37] have been proven to be very powerful tools for evaluating

* Corresponding author. Tel.: +82 32 860 7495; fax: +82 32 873 0181.
E-mail addresses: yongri.liang@umontreal.ca (Y. Liang), victoria821011@hotmail.com (M. Zheng), pkh1348@hanmail.net (K.H. Park), hslee@inha.ac.kr (H.S. Lee).
[1] Present address: Department of Chemistry, University of Montreal, PO Box 6128, Station Downtown, Montreal, QC H3C 3J7, Canada.

0032-3861/$ - see front matter © 2008 Elsevier Ltd. All rights reserved.
doi:10.1016/j.polymer.2008.02.012

surface structures and orientations of thin films of which the structure and especially their orientation at the surface of a thin polymer film were difficult to analyze with conventional transmittance WAXD and SAXS methods. Using GIWAXD technique, the characteristic behavior of the crystal structures of thin polymer films was extensively studied with poly(ethylene terephthalate) (PET) [20–22], polyimide [11,16], isotactic polypropylene (iPP) [12,13], poly(3-hexyl thiophene) (P3TH) [24,26], and polyfluorene [14].

Fourier transform infrared (FTIR) spectroscopy is an important technique for characterizing the localized chain structure in many polymers [38–40]. It can be used to probe subtle details such as intermolecular interactions, localized molecular conformations and orientations directly. Reflection absorption FTIR (RA-FTIR) spectroscopy is one of the various infrared techniques that are useful to characterize the structure in thin polymer films. With an incidence angle ranging from 75 to 88°, it is likely a good alternative for characterizing the physical structure of ultrathin films as the incident infrared radiation used for grazing incidence angle RA-FTIR spectroscopy spans a significantly wider surface area [41–45]. For the incidence angle given above, the illuminated surface area for RA-FTIR can be 3–30 times greater than the corresponding area analyzed in transmission FTIR with a normal incidence. One important characteristic of RA-FTIR is that the resultant electric field vector is perpendicular to the film surface when reflected from the metal substrate. Therefore, if molecules are adsorbed onto the substrate with a preferred orientation, vibration modes having transition moments perpendicular to the surface will appear with greater intensity than modes having transition moments parallel to the surface. Thus, RA-FTIR is especially useful for determining the orientation of molecular species in thin polymer films.

In this work, the crystal orientation of poly(trimethylene 2,6-napthalate) (PTN) films of various thicknesses was studied with synchrotron source GIXRD and grazing incidence RA-FTIR methods. The dependence of the crystal orientation on the film thickness was also examined.

2. Experimental section

2.1. Sample preparation

PTN synthesized with 1,3-propandiol and dimethyl 2,6-naphthalene dicarboxylate showed an intrinsic viscosity of 0.52 dL/g in a mixed solvent of 1,1,2,2-tetrachloroethane and phenol. The PTN was dissolved into a solvent of 1,1,1,3,3,3-hexafluoro-2-propanol to prepare PTN solutions of various concentrations. It was then spin-coated onto silicon (100) and gold-coated silicon wafers (Aldrich) (spin speed: 2000 rpm) for the GIWAXD and RA-FTIR measurements, respectively. The as-coated sample was baked in a vacuum oven at 40 °C for 12 h to remove residual solvent. To prepare an isotropic sample, the dried films were melted at 235 °C ($T_m = 204$ °C) for 3 min and then quickly quenched by liquid nitrogen-cooled air. The isothermally crystallized samples were prepared by isothermal annealing of the melt-quenched sample at 160 °C for 2 h. The thicknesses of cold-crystallized samples were measured with an ellipsometer (Plasmos Inc., SD2302 Model, with a wavelength of 632.8 nm He–Ne Laser) and by an Alpha-step device (DEKTAK3, Veeco Instruments Inc.). The sample thicknesses were the average values of both measurements.

2.2. 2D GIWAXD measurement and data analysis

The GIWAXD measurements were carried out at the 4C2 beamline of the PAL (Pohang Accelerator Laboratory, Korea) using a two-dimensional (2D) CCD detector (PI-SCX4300-165/2, Princeton Instruments). The wavelength of the incident X-rays was 1.54 Å and sample-to-detector distance was 126.8. Samples were mounted on a 4-circle kappa goniometer installed in a vacuum chamber. The incidence angle of the X-ray radiation was set to 0.24°. The critical angle of PTN was 0.171°.

One-dimensional (1D) in-plane and out-of-plane scan GIWAXD profiles were extracted from the corresponding 2D GIWAXD patterns [18,21]. The intensities of in-plane scan GIWAXD profiles were scanned along the horizontal direction while keeping the exit angle of 0.6° and the intensities of out-of-plane scan GIWAXD profiles were scanned along surface normal direction. To calculate average crystal orientation, the azimuthal scanning profiles of (002) reflection were extracted from corresponding 2D GIWAXD pattern. The intensities of azimuthal scanning profiles of (002) reflection were scanned along the azimuthal angle from −90 to 90° while keeping the 2θ of (002) reflection peak constant. The zero azimuthal angle was set to the meridional direction in the 2D GIWAXD pattern.

2.3. Grazing incidence reflection absorbance FTIR

To observe segmental orientations in thin films, the RA-FTIR spectra were measured with a variable-angle reflection accessory (Specac) and a polarizer-attached Bruker IFS 66v/s spectrometer using an incidence angle of 80° (angle from the plane normal). The polarization of the incoming beam was parallel to the plane of incidence (p-polarized).

3. Results and discussion

3.1. GIWAXD measurement

PTN is known to have two crystal structures known as the α and β forms. An α crystal can be obtained by cold crystallization whereas a β crystal structure is obtained by melt crystallization. The α-form PTN crystal is reported to have a monoclinic crystal system with unit cell parameters of $a = 0.722$ nm, $b = 0.709$ nm, $c = 2.384$ nm, $\alpha = 90.0°$, $\beta = 90.0°$, and $\gamma = 81.6°$ [46]. Although the detailed chain structure of the PTN β crystal has been previously reported, the chain conformation in the PTN α-form crystal has thus far not been reported [47].

Fig. 1 shows 2D GIWAXD patterns of isothermally crystallized PTN films with various film thicknesses. Fig. 2 shows two sets of one-dimensional GIWAXD profiles ((A) out-of-plane scan, (B) in-plane scan) which were obtained from the 2D GIWAXD patterns (Fig. 1). By combining the out-of-plane

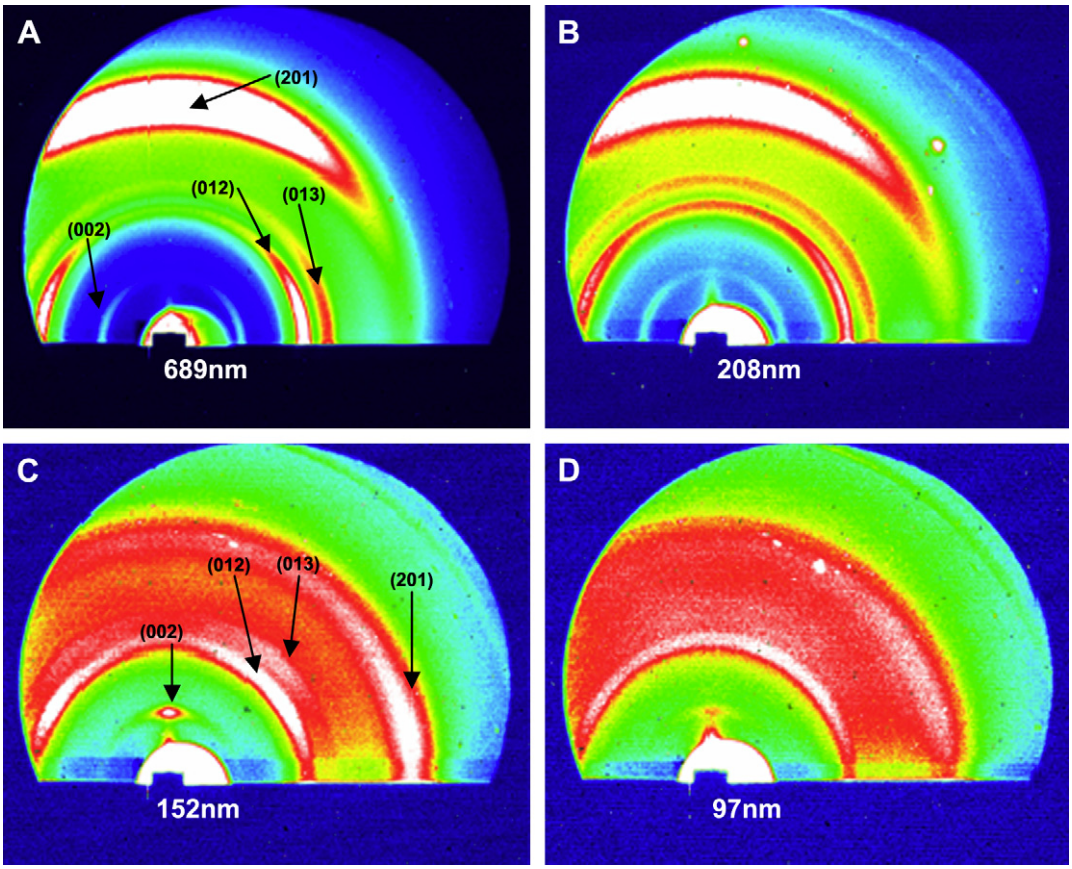

Fig. 1. 2D GIWAXD patterns of cold-crystallized PTN films of various thicknesses: (A) 689 nm (B) 208 nm (C) 152 nm and (D) 92 nm.

and in-plane scanning profiles of identical samples (Fig. 2(A), (B)), it was possible to confirm that the crystal structure of all samples is the α-form of PTN. Furthermore, the relative intensity of each diffraction peak in the out-of-plane scan is clearly different from that of the corresponding peak in the in-plane scan profile.

In the case of a thicker film (689 and 208 nm), the intensity of the (201) plane reflection in the out-of-plane scan is much stronger than that in the in-plane scan. Additionally, the intensities of the (011), (012) and (013) plane reflections were much weaker than the corresponding peaks in the in-plane scan profile; the reflection from the (002) plane can be observed clearly only in the in-plane scan profile. These results indicate that for a thicker film, the normal of (002) crystal plane is parallel to the sample surface. Furthermore, the "*a*" axis of the monoclinic unit cell, which is perpendicular to normal of the (002) crystal plane, is preferentially oriented nearly perpendicular to the film plane [23]. The orientation of the crystal on the surface is schematically shown in Fig. 3(A) for the thick film and in Fig. 3(B) for the thin film. In the α-form crystal unit cell, the angle between the "*c*" axis and normal to the (201) crystal plane is 81.2° and the angle between the "*b*" axis and normal to the (201) crystal plane is 90° [46]. Therefore, it can be also deduced that the "*c*" and "*b*" axes are nearly parallel to the film surface. The higher intensity of the (0*kl*) crystal planes in the in-plane scan is a direct indication of the preferential crystal orientation suggested above.

2D GIWAXD patterns of thinner samples (152 nm or thinner) are markedly different from those of thicker samples. The peak intensities from the crystal planes (201) and (0*kl*) are very different compared with those of a thicker sample. This fact indicates that the crystal orientation in a thin film is very different from that in a thicker film. The diffracted intensity from the (002) plane is clearly observed from the meridional direction and its intensity in the in-plane scan profile is negligible, as shown in Figs. 1(C), (D) and 2. This result implies that the chains in the α-form crystalline phase in a thin PTN film are nearly perpendicular to the film surface as shown schematically in Fig. 3(B). Based on the GIWAXD results, it can be suggested that the lamellae in a thick PTN film have an "edge-on" structure (Fig. 3(A)) whereas those in a thin film have a "flat-on" structure (Fig. 3(B)).

3.2. Crystal orientation function

In order to analyze crystal orientation quantitatively, the crystal orientation function was calculated using the method by Wilchinsy [48,49]. The azimuthal scanning profile of the (002) reflection was extracted from the corresponding 2D GIWAXD patterns and the results are shown in the Fig. 4. Azimuthal scanning profiles were used to calculate Herman's orientation function, f_c. The orientation function, f_c, was derived from the angle $\phi_{c,Z}$ between the main chain direction

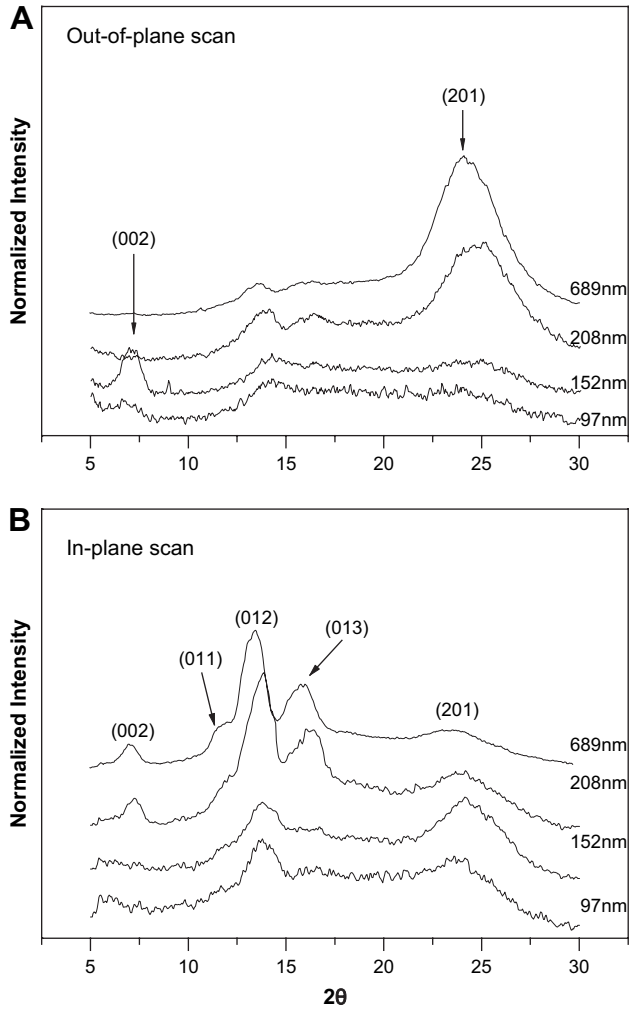

Fig. 2. (A) Out-of-plane scan profiles and (B) in-plane scan profiles of PTN samples of various thicknesses obtained from 2D GIWAXD patterns. The intensities were normalized by sample thickness.

((002) plane normal) and the normal direction of the thin film (reference direction (Z)), using Eq. (1) [50]

$$f_c = \frac{3\langle \cos^2 \phi_{c,Z} \rangle - 1}{2} = \frac{3\langle \cos^2 \phi_{002,Z} \rangle - 1}{2}. \quad (1)$$

Here, $\langle \cos^2 \phi_{c,Z} \rangle$ is the average value of the square of the cosine of the angle $\phi_{c,Z}$. The value of f_c ranges from -0.5 to 1 depending on the chain direction, which is either perpendicular or parallel with respect to the reference direction,

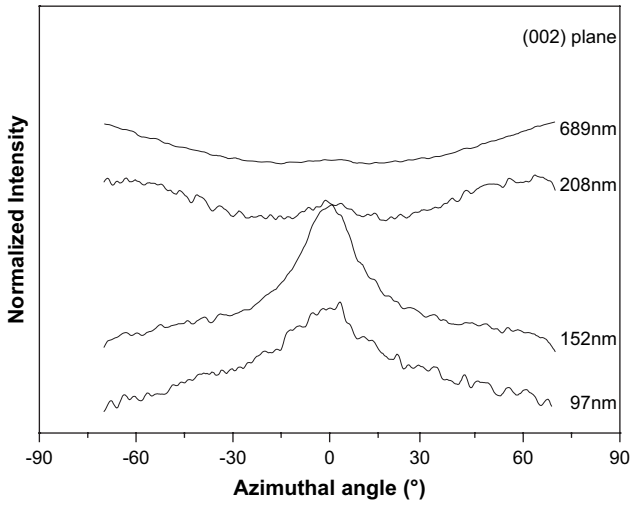

Fig. 4. Azimuthal scanning profiles of (002) reflection of samples with various thicknesses extracted from the corresponding 2D GIWAXD pattern. The intensities were normalized by sample thickness.

respectively. For a random orientation, f_c is zero. As the unit cell of the PTN α-form crystal has a monoclinic crystal system with $\beta = 90°$, the c-axis direction can be replaced with the (002) plane normal. Thus, the crystal orientation function f_c can be obtained with the second relationship in the Eq. (1).

Fig. 5 shows the crystal orientation function, f_c, with respect to the film plane normal as a function of the film thickness. In order to determine the crystal orientation of a bulk (~200 μm) sample, the 2D WAXS pattern illuminating the incidence X-ray along the film thickness direction was also measured. As expected, the crystal orientation function of the bulk sample becomes zero, indicating the isotropic orientation of the crystal in the bulk sample. For thicker films (689 and 208 nm), the crystal orientation function shows a negative value whereas with thinner films (98 and 152 nm) it shows a positive value. These results clearly indicate that the crystal orientation is strongly dependent on the sample thickness. Furthermore, the polymer chain axis in the crystalline phase of the thicker films is preferentially parallel with the film surface (Fig. 3(A)), whereas it is preferentially perpendicular in the case of the thinner films (Fig. 3(B)).

In a previous work by the authors with a PTN bulk film (~200 μm thick), the chain orientation at the film surface was studied with the polarized FTIR-ATR method during the cold crystallization of a melt-quenched PTN film [23]. Upon

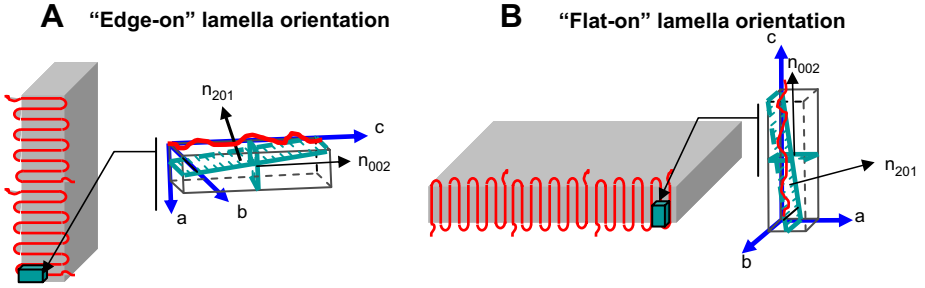

Fig. 3. Schematic illustration for the surface crystal orientation. (A) Edge-on lamella orientation, (B) flat-on lamella orientation. n_{hkl} is normal vector of (hkl) plane.

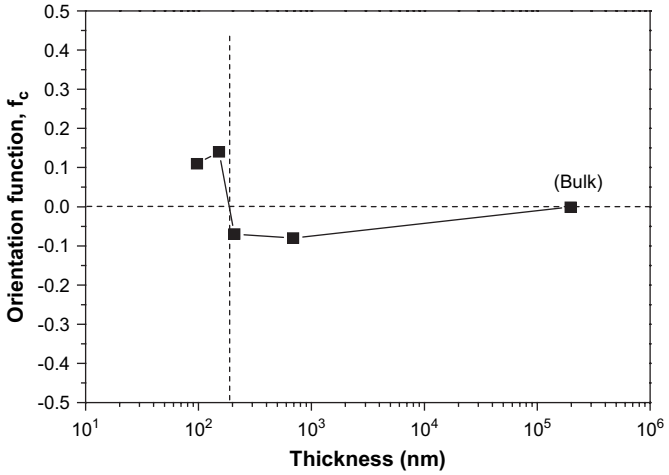

Fig. 5. The crystal orientation function, f_c, as a function of the sample thickness.

cold crystallization, the random orientation of the chains in the melt-quenched film was found to transform into an anisotropic orientation due to the surface-induced crystallization. Furthermore, the chains in the crystalline phase in the surface region monitored by FTIR-ATR spectroscopy were found to be parallel with the surface, and the naphthalene rings also became flat at the surface. These FTIR-ATR results are consistent with the GIWAXD results from Figs. 1 and 2 for the thicker films.

3.3. Reflection absorption FTIR measurement

In order to investigate the segment orientation and its dependence on the film thickness in PTN samples, the RA-FTIR spectra were obtained. Fig. 6 shows the RA-FTIR spectra of PTN samples of various thicknesses as prepared by (B) melt-quenching and (A) isothermal crystallization at 160 °C for 2 h. The bands primarily studied in this work are noted with arrows in Fig. 5. The band at 1602 cm^{-1} is associated with the C=C stretching mode in the naphthalene ring and bands at 917 and 765 cm^{-1} are related to the out-of-plane bending mode of C–H groups in naphthalene ring. The transition moment of the band at 1602 cm^{-1} is "parallel", and the others are "perpendicular" to the naphthalene ring plane. In the RA-FTIR experiment, the electric field of the infrared radiation reflected by the metal surface is perpendicular to the film surface provided that the film thickness is sufficiently thinner compared with the wavelength of the incident infrared radiation [51]. Therefore, the absorbance ratio of "perpendicular" (1602 cm^{-1}) and "parallel" bands (917 and 765 cm^{-1}) can be used to estimate the naphthalene ring orientation in the film.

Fig. 7 shows the ratio, R, of the absorbance of the 917 cm^{-1} band to that of the 1602 cm^{-1} band as a function of the film thickness of the isothermally crystallized and melt-quenched PTN films. For the melt-quenched samples, the absorbance ratio increases gradually with the film thickness up to nearly 350 nm, and then slightly decreases. For the isothermally crystallized samples, however, very different results were observed. For the thinner films, the absorbance ratio value of the isothermally

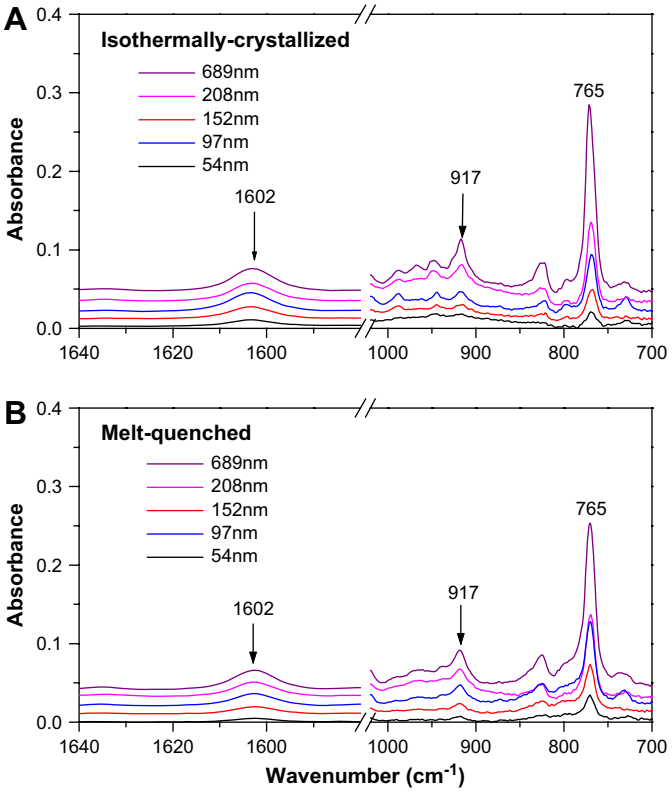

Fig. 6. RA-FTIR spectra of various thicknesses of PTN samples as prepared by (A) isothermal crystallization at 160 °C for 2 h and (B) melt-quenching.

crystallized sample was very low compared to the corresponding value of the melt-quenched sample. Additionally, it remains as a very low value as the film thickness increases to 200 nm (region A). The ratio increases abruptly as the film thickness increases further to nearly 350 nm (region B), and its value maintains high.

It should be noted that the electric field of the infrared radiation for grazing incidence RA-FTIR experiment with a thin polymer film is perpendicular to the sample surface. The low ratio value for the thinner film of the isothermally crystallized sample, therefore, can be interpreted in terms of the perpendicular orientation of the naphthalene rings and the polymer chains to the film surface, as in the "flat-on" orientation of the lamellae (Fig. 3(B)). For the film with an "edge-on" lamellar orientation (Fig. 3(A)), the chain and the naphthalene rings in the crystal will be parallel to the surface, resulting in the high and low absorbance of the 917 and 1602 cm^{-1} peaks, respectively (Fig. 7). The high ratio value of the isothermally crystallized sample in the (B) region in Fig. 7 can be, therefore, interpreted in terms of the "edge-on" orientation of the lamellae in the thicker film. The lamellar orientation deduced from the grazing incidence RA-FTIR result is consistent with that from the GIWAXD results. Furthermore, the flat orientation of the naphthalene rings in the crystalline phase of the thicker film was suggested in a previous work involving FTIR-ATR with a cold-crystallized PTN film [23].

Although the ratio of the isothermally crystallized sample showed a drastic change at a thickness of approximately 200 nm, this change with the melt-quenched sample is not negligible as well. Either the melting process used in this

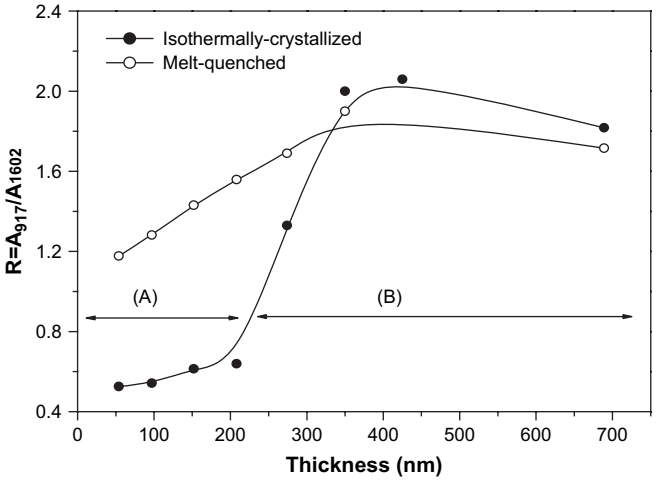

Fig. 7. Absorbance ratios of the 917 and 1602 cm^{-1} band as a function of the film thickness. ○, Melt-quenched sample; •, isothermally crystallized sample.

work may not be sufficient to completely remove any anisotropy introduced during the spin-coating process, or there is inherent anisotropy in a certain fraction of the film having direct contact with air or the substrate surface. Further studies should be carried out to elucidate more clearly the exact origin of the thickness dependence of the ratio *R* for a melt-quenched film.

4. Conclusions

In this work, the crystal orientation in isothermally crystallized PTN film and its dependence on the film thickness were studied with 2D GIWAXD and RA-FTIR methods. Grazing incidence RA-FTIR was found to be very useful to monitor the segmental orientation in thin polymer films.

It was found that the crystal orientation is strongly dependent on sample thickness and that its orientation shows a significant difference for the film thickness of the PTN film above and below approximately 200 nm. By analyzing in-plane and out-of-plane scans of the 2D GIWAXD profiles and the relative absorbance of the parallel and perpendicular peaks of RA-FTIR, it can be concluded that for films thinner than 200 nm, the polymer chains in the crystalline phase of the isothermally crystallized PTN show a preferential orientation that is perpendicular to the film plane, whereas for a thick film those are parallel to the film surface. Furthermore, the naphthalene rings in the crystalline phase of the thick film was also found to be flat on the film surface, which is consistent with previous FTIR-ATR results [23]. The chain orientations found in this work can be explained in terms of the ''edge-on'' and ''flat-on'' orientations of the lamellar crystals generally observed for thick and thin films, respectively, in other polymer systems [23].

Acknowledgment

This work was supported by an INHA University Research Grant. The GIWAXD experiment at PLS in Korea was supported by MOST and POSCO in Korea.

References

[1] Frank CW, Rao V, Despotopoulou MM, Pease RFW, Hinsberg WD, Miller RD, et al. Science 1996;273:912–5.
[2] Hietpas GD, Sands JM, Allara DL. J Phys Chem B 1998;102(51):10556–67.
[3] Yang X, Shi J, Johnson S, Swanson B. Langmuir 1998;14:1505–7.
[4] Liang T, Makita Y, Kimura S. Polymer 2001;42(11):4867–72.
[5] Walheim S, Schäffer E, Mlynek J, Steiner U. Science 1999;283:520–2.
[6] Kim JH, Jang J, Zin W-C. Langmuir 2001;17:2703–10.
[7] Despotopoulou MM, Frank CW, Miller RD, Rabolt JF. Macromolecules 1996;29(18):5797–804.
[8] Schonherr H, Frank CW. Macromolecules 2003;36:1188–98.
[9] Wang Y, Ge S, Rafailovich M, Sokolov J, Zou Y, Ade H, et al. Macromolecules 2004;37(9):3319–27.
[10] Schonherr H, Frank CW. Macromolecules 2003;36:1199–208.
[11] Factor BJ, Russell TP, Toney MF. Macromolecules 1993;26:2847–59.
[12] Kawamoto N, Mori H, Nitta K-h, Sasaki S, Yui N, Terano M. Macromol Chem Phys 1998;199:261–6.
[13] Kawamoto N, Mori H, Nitta K-h, Yui N, Terano M. Angew Makromol Chem 1998;256:69–74.
[14] Kawana S, Durrell M, Lu J, Macdonald JE, Grell M, Bradlely DDC, et al. Polym Bull 2002;43:1907–13.
[15] Murthy NS, Bednarczyk C, Minor H. Polymer 2000;41:277–84.
[16] Saraf RF, Dimitrakopoulos C, Toney MF, Kowalczyk SP. Langmuir 1996;12:2802–6.
[17] Yakabe H, Sasaki S, Sakata O, Takahara A, Kajiyama T. Macromolecules 2003;36:5905–7.
[18] Yakabe H, Tanaka K, Nagamura T, Sasaki S, Sakata O, Takahara A, et al. Polym Bull 2005;53:213–22.
[19] Zhang Y, Mukoyama S, Mori K, Shen D, Yan S, Ozaki Y, et al. Surf Sci 2006;600:1559–64.
[20] Macdonald JE, Durell M, Trolley D, Lei C, Das A, Jukes PC, et al. Radiat Phys Chem 2004;71:811–5.
[21] Jukes PC, Das A, Durell M, Trolley D, Higgins AM, Geoghegan M, et al. Macromolecules 2005;38(6):2315–20.
[22] Durell M, Macdonald JE, Trolley D, Wehrum A, Jukes PC, Jones RAL, et al. Europhys Lett 2002;58(6):844–50.
[23] Liang Y, Lee HS. Macromolecules 2005;38(23):9885–8.
[24] Yang H, Kim SH, Yang L, Yang SY, Park CE. Adv Mater 2007;19:2868–72.
[25] Yoon J, Jin KS, Kim HC, Kim G, Heo K, Jin S, et al. J Appl Crystallogr 2007;40:476–88.
[26] Kim Y, Cook S, Tuladhar SM, Choulis SA, Nelson J, Durrant JR, et al. Nat Mater 2006;5:197–203.
[27] Park I, Lee B, Ryu J, Im K, Yoon J, Ree M, et al. Macromolecules 2005;38:10532–6.
[28] Lazzari R. J Appl Crystallogr 2002;35:406–21.
[29] Lee B, Oh W, Hwang Y, Park Y-H, Yoon J, Jin KS, et al. Adv Mater 2005;17:696–701.
[30] Lee B, Oh W, Yoon J, Hwang Y, Kim J, Landes BG, et al. Macromolecules 2005;38:8991–5.
[31] Lee B, Park Y-H, Hwang Y-T, Oh W, Yoon J, Ree M. Nat Mater 2005;4:147–51.
[32] Tate MP, Urade VN, Kowalski JD, Wei T-c, Hamilton BD, Eggiman BW, et al. J Phys Chem B 2006;110:9882–92.
[33] Kim J-S, Kim H-C, Lee B, Ree M. Polymer 2005;46(18):7394–402.
[34] Lee B, Park I, Yoon J, Park S, Kim J, Kim K-W, et al. Macromolecules 2005;38:4311–23.
[35] Lee B, Yoon J, Oh W, Hwang Y, Heo K, Jin KS, et al. Macromolecules 2005;38:3395–405.
[36] Heo K, Oh KS, Yoon J, Jin KS, Jin S, Choi CK, et al. J Appl Crystallogr 2007;40:s614–9.
[37] Heo K, Park S-G, Yoon J, Jin KS, Jin S, Rhee S-W, et al. J Phys Chem C 2007;111:10848–54.
[38] Vasanthan N, Salem DR. Macromolecules 1999;32:6319–25.
[39] Zhang J, Duan Y, Sato H, Tsuji H, Noda I, Yan S, et al. Macromolecules 2005;38:8012–21.
[40] Zhang J, Tsuji H, Noda I, Ozaki Y. Macromolecules 2004;37:6433–9.

[41] Parikh AN, Allara DL. J Chem Phys 1992;96:927–45.
[42] Zhang Y, Zhang J, Lu Y, Duan Y, Yan S, Shen D. Macromolecules 2004;37:2532–7.
[43] Jin XY, Kim KJ, Lee HS. Polymer 2005;46(26):12410–5.
[44] Lee SW, Chae B, Hahm SG, Lee B, Kim SB, Ree M. Polymer 2005;46(12):4068–76.
[45] Lee SW, Chae B, Kim HC, Lee B, Choi W, Kim SB, et al. Langmuir 2003;19:8735–43.
[46] Jeong YG, Jo WH, Lee SC. Polymer 2003;44(11):3259–67.
[47] Jeong YG, Jo WH, Lee SC. Polymer 2004:379–84.
[48] Wilchinsky ZW. Advances in X-ray analysis. New York: Plenum Press; 1963.
[49] Alexander LE. X-ray diffraction methods in polymer science. New York: John Wiley & Sons. Inc.; 1969.
[50] Gedde UW. Polymer physics. London: Chapman & Hall; 1995.
[51] Greenler RE. J Chem Phys 1966;44:310–5.